Ultrasensitivity in multisite phosphorylation of membrane-anchored proteins.

Omer Dushek[†,‡,¶], P. Anton van der Merwe[†], Vahid Shahrezaei[§,¶]

[†]Sir William Dunn School of Pathology, University of Oxford
[‡]Centre for Mathematical Biology, University of Oxford
[§]Department of Mathematics, Imperial College
[¶]Corresponding authors

Corresponding authors.
Omer Dushek, Sir William Dunn School of Pathology
University of Oxford, South Parks Road, Oxford, OX1 3RE, United Kingdom
P: +44 01865 285497, E: omer.dushek@path.ox.ac.uk

Vahid Shahrezaei, Department of Mathematics
Imperial College, South Kensington Campus, London, SW7 2AZ, United Kingdom
P: +44 02075 948516, E: v.shahrezaei@imperial.ac.uk

Running title. Ultrasensitivity in membrane proteins

Key words. multisite phosphorylation, ultrasensitivity, diffusion-limited reactions, membrane-confined reactions

Abstract

Cellular signaling is initially confined to the plasma membrane where the cytoplasmic tails of surface receptors and other membrane-anchored proteins are phosphorylated in response to ligand binding. These proteins often contain multiple phosphorylation sites which are regulated by membrane-confined enzymes. Phosphorylation of these proteins is thought to be tightly regulated because they initiate and regulate signaling cascades leading to cellular activation, yet how their phosphorylation is regulated is poorly understood. Ultrasensitive or switch-like responses in their phosphorylation state are not expected because the modifying enzymes are in excess. Here we describe a novel mechanism of ultrasensitivity exhibited by multisite membrane-anchored proteins, but not cytosolic proteins, even when enzymes saturate the substrate. The mechanism underlying this concentration-independent ultrasensitivity is the local saturation of a single enzyme by multiple sites on the substrate. Local saturation is a passive process arising from slow membrane diffusion, steric hindrances, and multiple sites, and therefore may be widely applicable. Critical to this ultrasensitivity is the brief enzymatic inactivation that follows substrate modification. Computations are presented using ordinary-differential-equations and stochastic spatial simulations. We propose a new role for multisite membrane-anchored proteins, discuss experiments that can be used to probe the model, and relate our findings to previous theoretical work.

Introduction

Cellular signaling relies on post-translational modifications of proteins to integrate and shape the transmission of extracellular information into functional cellular outcomes. Phosphorylation and dephosphorylation of serine, threonine or tyrosine residues on proteins by kinases and phosphatases, respectively, can impact signal transmission by altering the localization, enzymatic activity, and interaction partners of a protein. Interestingly, the phosphorylation state of proteins in individual cells can be very sensitive to upstream stimuli, so that small changes in stimulus (e.g. active kinase, receptor occupancy, etc) can result in large changes in the phosphorylation. Examples of such ultrasensitive or switch-like responses in intracellular proteins are well documented (1–7), and are thought to be critical for cellular decision-making processes.

The processing of extracellular information is initially confined to the plasma membrane, where the cytoplasmic tails of receptors and other membrane-anchored proteins become phosphorylated, typically on multiple tyrosines residues. These phosphorylated residues serve as docking sites for enzymes which, when bound, propagate cellular signaling by catalyzing additional reactions. As an example, consider a class of cell surface receptors that include antigen, Fc, and other immune receptors, which contain conserved tyrosine-containing motifs, such as immunoreceptor tyrosine-based activation, inhibitory, and switch motifs, termed ITAMs, ITIMs, and ITSMs, respectively (8–10). In contrast to receptor tyrosine kinases (RTKs) (11), these receptors do not contain intrinsic catalytic domains and are regulated by extrinsic membrane-anchored tyrosine kinases and phosphatases (10). We refer to these receptors as non-catalytic tyrosine-phosphorylated receptors (NTRs). Like other receptors, the phosphorylation of NTRs directly impacts cellular decisions by initiating and regulating intracellular signaling cascades, yet how their phosphorylation is regulated by extrinsic enzymes is poorly understood.

As a representative NTR, consider the T cell antigen receptor (TCR). The TCR is a multi-subunit receptor on the surface of T cells that contains 20 phosphorylation sites distributed on 10 ITAMs (12). Each ITAM contains two tyrosine residues that are phosphorylated by the Src family kinase Lck and dephosphorylated by the phosphatase CD45, both of which are also confined to the plasma membrane. The phosphorylation state of the TCR is thought to be tightly regulated because the intracellular signaling cascade initiated by phosphorylated TCR ITAMs leads to T cell activation, which if inappropriate, can result in autoimmune disorders (12). Many NTRs contain multiple phosphorylation sites (8) and in the case of the TCR, the large number of sites are thought to be primarily required for signal amplification (12). A switch-like response at the level of individual NTRs can be useful for reducing noise and maintaining signal fidelity and in the case of antigen receptors, it can contribute to the discrimination of antigens (13). In addition to NTRs, many non-receptor membrane-confined molecules, such as the adaptor Linker for Activated T cells (LAT), contain multiple phosphorylation sites that are regulated by membrane confined enzymes.

The mechanisms underlying switch-like responses in the phosphorylation state of proteins are incompletely understood. For the case of a cytosolic protein containing a single phosphorylation site, Goldbeter and Koshland (14) mathematically showed that small changes in the active kinase or phosphatase concentrations can result in dramatic changes to the phosphorylation state of the protein. Since this sensitivity relies on the enzymes operating in the zero-order regime (where the concentrations of substrate is in excess of the enzyme concentrations), it was termed zero-order ultrasensitivity. Although an attractive explanation, zero-order ultrasensitivity has rarely been the mechanism for the observed switch-like response in cellular signaling because enzymes often operate outside of the zero-order regime. In some cases, additional mechanisms (e.g. feedbacks (6), competition (4)) have been shown to be responsible for the switch-like

response.

As for many cytosolic proteins, the enzymes acting on membrane-anchored proteins are also in excess. For the case of the T cell antigen receptor, the phosphatase CD45 is the most abundant cell surface protein on T cells and the kinase Lck is at least twice as abundant as the TCR (2). Therefore, enzymatic modifications are expected to be operating outside of the zero-order regime. An important difference between cytosolic and membrane-anchored proteins is their respective mobilities, whereas diffusion coefficients of cytosolic proteins are in the range of 1-10 μm^2/s the diffusion coefficients of membrane proteins are in the range of 0.01-0.1 μm^2/s. Therefore, it is commonly believed that the coupling of proteins in the membrane is limited by diffusion (15).

In this work, we report a novel mechanism of ultrasensitivity exhibited by multisite membrane-anchored proteins, but not cytosolic proteins, that operates in the first order regime. Using detailed mathematical modeling, we examine the effect of changes in the kinase-phosphatase balance on the phosphorylation of multisite membrane-anchored proteins when enzymes operate in the first-order regime (i.e. enzymes are globally in excess of substrate) and find impressive ultrasensitivity that increases with the number of phosphorylation sites. Critical to this ultrasensitivity is the explicit modeling of diffusion-limited reactions and brief enzymatic inactivation that follows catalysis. All results are initially presented using a computationally efficient ordinary-differential-equation (ODE) model but key results are recapitulated using a stochastic spatial simulator. We propose a new role for multisite membrane-anchored proteins (such as NTRs), discuss experiments that can be used to probe the model, and relate our findings to previous theoretical work.

Results

A two-step model captures the effects of membrane diffusion.

We begin exploring the effects of membrane diffusion on substrate phosphorylation using a two-step model (15–17) (Fig. 1A-B),

$$S_j \underset{k_-}{\overset{Xk_+}{\rightleftharpoons}} X\cdot\cdot S_j \underset{k_{\text{off}}}{\overset{k^*_{\text{on}}}{\rightleftharpoons}} XS_j \tag{1}$$

where S_j is the free substrate concentration having j-sites phosphorylated and X is the free enzyme concentration ($X = E$ for kinase, $X = F$ for phosphatase). In this model, the enzyme and substrate must first form an encounter complex ($X\cdot\cdot S_j$) before binding (XS_j). The rate of forming an encounter complex is Xk_+ where k_+ is the diffusion-limited on-rate (see below). The encounter complex represents an approximate state where the enzyme and substrate are unbound but within physical proximity such that binding can take place. In this state, the molecules bind (k^*_{on}) or move apart (k_-) with first order rates. When bound to the substrate, the enzyme may catalyze a reaction and dissociate (k_{r}, not shown in above scheme) or dissociate (k_{off}). Both k_{r} and k_{off} reactions result in an encounter complex and therefore the model locally captures Michelis-Menten kinetics.

When the substrate is free of enzyme (S), the rate at which enzyme binds (or couples) is $k_c = k_+k^*_{\text{on}}/(k^*_{\text{on}}+k_-)$ and when the substrate is bound to enzyme (SX), the rate at which it fully unbinds (or uncouples) from enzyme is $k_u = k_{\text{off}}k_-/(k^*_{\text{on}} + k_-)$. At equilibrium we expect that $K_{\text{D}} = k_{\text{off}}/k_{\text{on}}$ and therefore

$k_u/k_c = k_{off}/k_{on}$. Assuming that $k^*_{on} = k_{on}/A$, where A is the encounter area (i.e. $1/A$ is the effective local concentration), it then follows that $k_- = k_+/A$. Therefore, the local rates (k_-, k^*_{on}) govern the interaction between a single enzyme and substrate but are directly related to the macroscopic bimolecular rates (k_+, k_{on}): $k_- = k_+/A$ and $k^*_{on} = k_{on}/A$. Note that the two step ODE model includes both the diffusion and binding steps and therefore the parameters k_c and k_u do not explicitly appear. Parameter definitions are summarized in Table 1.

The diffusion-limited on-rate on the membrane is $k_+ = 2\pi D/\log(b/s)$ (15–17), where $D = D_X + D_S$ is the sum of the diffusion coefficients for the enzyme (D_X) and substrate (D_S), b is the mean distance between enzyme ($b \approx 1/\sqrt{\pi X}$), and s is the reaction radius. A typical membrane protein is on the scale of 10 nm ($s = 0.0056$ μm, $A = \pi s^2 = 10^{-4}$ μm^2) and enzyme concentrations are in excess of 100 μm^{-2} ($b = 0.056$ μm). Taking the membrane diffusion coefficients to be $D_S = D_E = D_F = 0.01$ μm^2/s (18) we find that $k_+ \approx 0.05$ μm^2/s.

The model contains several assumptions. First, it is assumed that enzymes are in excess over substrate and therefore the model is completely linear (i.e. enzymes operate far from the zero-order regime). Second, we initially assume that only a single enzyme can be within the encounter complex (e.g. due to steric effects) but we later relax this assumption. Third, we assume enzymes act distributively, so that dissociation from the substrate occurs before subsequent catalytic modifications. Lastly, we present all results using a random phosphorylation scheme and complete parameter symmetry for the kinase and phosphatase. Sequential phosphorylation does not alter any of our conclusions. The most general model we consider consists of 143 coupled ODEs which are generated using BioNetGen (19) and integrated in Matlab (Mathworks, MA). We include the BioNetGen file used to generate the ODE system in the Supplementary Materials. As output from the model we compute the normalized total phosphorylation of the substrate at equilibrium,

$$\langle S \rangle = \sum_{j=0}^{N} j(S_j + E \cdot \cdot S_j + ES_j + F \cdot \cdot S_j + FS_j)/(NS_T) \tag{2}$$

where N is the number of sites and S_T is the total substrate concentration. The key advantage of using this approximate two-step model instead of explicit spatial simulations is that the former is computationally efficient.

Effective processivity via membrane diffusion.

In Fig. 2A we first show $\langle S \rangle$ as a function of the E/F-ratio for substrates with 1-20 phosphorylation sites in the reaction limited regime ($k_{on} = k_+/100$). In this limit, the two-step ODE model reduces to the classical well-mixed single-step model. We observe subsensitivity for the single site substrate which is reduced with increasing sites. This subsensitivity has been previously observed (20) and arises in the dilute substrate limit when enzymes interact with the substrate with high affinity. In this regime, the quasi-steady state assumption is violated and full model calculations that explicitly track the substrate-enzyme complex (as we have performed) or the total quasi-steady state approximation is required (20). Subsensitivity is reduced in substrates with multiple phosphorylation sites but as expected, ultrasensitivity is not observed (Fig. 2A inset) because enzymes are not saturated (i.e enzymes are operating far from the zero-order regime). Additional details on subsensitivity can be found in the Supplementary Information.

We reasoned that multisite substrates will provide local enzymatic saturation in the diffusion-limited

regime ($k_{\text{on}} = 100k_+$) since in the encounter complex there is a single enzyme and multiple phosphorylation sites. However, in this regime the phosphorylation state of the substrate is not sensitive to large changes in the E/F-ratio (Fig. 2B). This follows from the observation that a single enzyme-substrate encounter leads to multiple modifications (via rebinding) (21) and therefore diffusion-limited rates provide effective processivity (despite distributive enzyme kinetics), attenuating the dependence of substrate phosphorylation on enzyme concentrations. In other words, the dose-response curves for multisite substrates collapse onto the single site substrate curve. Allowing multiple enzymes to form an encounter-complex with the substrate reduces the effects of processivity (see section on volume exclusion and Fig. S3 in Supplementary Information).

Ultrasensivity by multisite phosphorylation and enzymatic inactivation.

Processivity occurs because the rate of binding (k^*_{on}) is much larger than the local diffusive rate (k_-) for membrane reactions. On these fast timescales, which we approximate to be $1/k^*_{\text{on}} \sim 0.01$ ms and $1/k_- \sim 1$ ms (see Fig. 2), processes may take place that prevent the enzyme and substrate from rebinding. For example, the addition of a phosphate to the substrate leaves the kinase with an attached ADP which must be converted to ATP (directly or via release of ADP and re-attachment of ATP) before the kinase can bind and catalyze an additional reaction (21–23). To model such processes we include a short refractory period (Fig. 1C) during which substrate and enzyme cannot bind by introducing a first order rate μ capturing the rate of enzymatic re-activation. Repeating the computation with $\mu = 1$ s^{-1} we find no change in the reaction-limited regime (Fig. 2C) but impressive ultrasensivity in the diffusion-limited regime (Fig. 2D) that improves with the number of phosphorylation sites.

To further emphasize the relative role of diffusion, binding, and inactivation, we show the Hill numbers as a function of these parameters for a 20-site protein in Fig. 3. In Fig. 3A we observe that longer refractory periods (smaller values of μ) and slower diffusion (i.e. smaller values of k_+, and therefore smaller values of k_-) lead to larger Hill numbers. We note that an optimum k_- emerges (e.g. when $\mu = 1$ s^{-1}) because when $k_- \lesssim \mu$ processivity is frequent and when $k_- > 1000$ s^{-1} the reaction is no longer diffusion-limited. This latter point is illustrated in Fig. 3B, where we observe large Hill numbers only in the diffusion-limited regime (lower right quadrant). Therefore ultrasensivity is possible only when $k^*_{\text{on}} > k_- > \mu$. In other words, reactions must be limited by diffusion ($k^*_{\text{on}} > k_-$) but diffusion must be sufficiently large so that enzymes only re-activate after moving away from the substrate ($k_- > \mu$). Additionally, we find that ultrasensitivity is possible over a wide range of k_{off} and k_{r} provided that the probability of an enzymatic modification ($k_{\text{r}}/(k_{\text{r}} + k_{\text{off}})$) is no smaller than $\sim$0.01 (Fig. 3C).

In summary, individual multisite proteins can act as switches even in the dilute substrate limit when reactions are diffusion-limited and when modeling the short refractory period of enzymes. In what follows we reproduce key results using a stochastic spatial simulator and explore the effects of volume exclusion.

Effects of volume exclusion in explicit spatial simulations

The above results are obtained with a computationally efficient but approximate ODE system based on the two-step model (15–17) (Fig. 1). To confirm that the observed ultrasensitivity is not an artifact of the approximative nature of the two-step ODE model, it is important to reproduce our results using explicit spatial

simulations. To do this, we utilized Smoldyn, a Monte Carlo particle-based spatial simulator that captures local rebinding effects accurately (24) (see Methods). As in the ODE model, we implemented the enzymatic modification (without any quasi steady-state simplifications) of a diffusing kinase and phosphatase acting on a multisite substrate and explicitly imposed volume exclusion between enzymes in order to account for steric effects (enzymes are modeled as hard discs with an 'exclusion' radius of 5 nm, see Methods). In all simulations we fix the binding radius to 5 nm. We note that complete enzyme exclusion is implicit in the two-step ODE model because only a single enzyme can form an encounter complex with the substrate at any given time.

The Smoldyn simulations reproduced the results obtained with the two-step ODE model. We observed ultrasensitivity that is dependent on the number of phosphorylation sites (Fig. 4A) and as expected, removing the refractory period or increasing the diffusion coefficient so that reactions are no longer limited by diffusion abolishes the observed ultrasensitivity (Fig. 4B).

We next investigated the effects of volume exclusion. We observed that removing volume exclusion, by setting the exclusion radius to 0 nm, increases the number of enzymes that can simulatenously interact with the substrate resulting in reduced ultrasensitivity (Fig. 4B,C). Similarily, in a modified two-step ODE model that allows more than one enzyme to form an encounter complex with the substrate, we also observed reduced ultrasensitivity (see Supplementary Information and Fig. S3). The presence of multiple enzymes within the reaction radius reduces the ratio of sites to enzymes and therefore locally decreases the saturation of enzymes by sites. Together with the observation that increasing the number of sites can compensate for multiple enzymes within the reaction radius (Fig. 4B), we conclude that the observed ultrasensitivity critically depends on local enzymatic saturation. Indeed, increasing the exclusion radius to 25 nm in the Smoldyn simulations, so that only a single enzyme can interact with the substrate, we recover Hill numbers comparable to the ones obtained from the ODE model (Fig. 4C).

In summary, explicit spatial simulations in Smoldyn qualitatively reproduce both the ultrasensitivity observed in the approximate two-step ODE model and the conditions for such ultrasensitivity. Quantitative agreement is not possible because the more realistic spatial simulations in Smoldyn, where both the exclusion and binding radii are set to 5 nm, allow multiple enzymes within the reaction radius of the substrate whereas the two-step ODE model does not. We note that ultrasensitivity in multisite substrates does not come about from any concentration effects because, for example, simulations with 20 single site substrates do not produce ultrasensitivity (not shown) whereas simulations with a single 20-site substrate do (Fig. 4A).

Discussion

In this work, we have shown that ultrasensitivity can arise in multisite proteins by local enzymatic saturation and enzyme inactivation. Local saturation is established by purely passive processes. Steric hindrances and slow membrane diffusion result in a situation where a single enzyme is locally saturated by multiple phosphorylation sites. Consistent with this mechanism, allowing multiple enzymes within the reaction radius, increasing the diffusion coefficient, or reducing the number of sites can decrease (and, in the appropriate limits, abolish) the observed ultrasensitivity. Brief enzymatic inactivation maintains distributive kinetics which have been previously shown to be important for switch-like responses (25). Importantly, all calculations have been performed in the limit where enzymes globally saturate the substrate and therefore the observed ultrasensitivity is not a result of the classic zero-order mechanism.

Relation to previous work. The majority of studies use simple ODEs to model biochemical systems and therefore assume that the system is well-mixed. This assumption fails to capture the local spatio-temporal correlations present when the coupling rate between enzyme and substrate is, at least partially, dependent on diffusion. For example, Takahashi et al (21) have recently shown that enzyme-substrate rebinding can convert a distributive mechanism into a processive mechanism, which can result in the loss of bistability. Since rebinding events are not captured by well-mixed ODE models, computationally expensive spatial simulations are thought to be required. Here, we have used a two-step ODE model that explicitly models the encounter complex (Fig. 1) to capture rebinding events. This model was previously shown to agree with spatial simulations in the dilute substrate limit (26) and we have repeated the findings of the two-step ODE model using spatial simulations in Smoldyn. The key advantage of the two step ODE model, over spatial simulations, is that it can be used to rapidly explore parameter space, as in Fig. 3. We note that the one-step diffusion-limited ODE model, which does not explicitly include the encounter-complex, cannot approximate the effects of membrane diffusion (see Supplementary Materials), as previously reported by Takahashi et al (21).

In a recent study of the yeast mating pathway, Malleshaiah et al (7) reported a novel mechanism of ultrasensitivity based on local enzymatic saturation that is achieved by two-stage binding. Enzymes in their cytosolic signaling module first bound the substrate using a binding domain (stage 1) and only then were they able to bind one of the multiple phosphorylation sites to catalyze a reaction (stage 2). In the present work, we have shown that slow membrane diffusion is able to effectively create two binding steps and therefore enzymes are not required to have a second binding domain. In this way, our proposed ultrasensitivity mechanism should be applicable to a wide range of systems.

The present mechanism of ultrasensitivity is robust to variations in protein concentrations (total substrate - enzyme ratio) because it can operate outside of the zero-order regime. In this first-order regime, multisite phosphorylation has been shown to support switch-like responses when including additional effects such as cooperativity between sites or between sites and the enzymes (27), non-essential sites (28), conformational changes (27), substrate sequestration (29), entropic mechanisms (30), and cascades of enzymes (31). We have shown that, at least for membrane-anchored proteins, multiple sites are sufficient to give switch-like resposnes. Previous reports of bistability (32) and multistability (33) in multisite phosphorylation rely, in part, on zero-order kinetics. Our work suggests that multistability may be possible even in the dilute substrate limit.

Model parameters. The ultrasensitivity we have described depends on the parameter regime of the system, namely that $k^*_{\text{on}} > k_- > \mu$ (Fig. 3), and therefore it is important to determine whether this regime is physiologically relevant. The first inequality imples that $k_{\text{on}} > k_+$ or in other words, that the bimolecular reaction on-rate is larger than the diffusion-limited on-rate which is directly proportional to the diffusion coefficient. Estimates of diffusion coefficients are available (e.g. $D = 0.05$ μm^2/s for the T cell receptor (18)) but little information is available on the *in situ* reaction rates. Fluorescence recovery after photobleaching (FRAP) has been previously used to determine the reaction rates between cytosolic proteins (34) and a protocol has been proposed to determine reaction rates for membrane-confined proteins (35). In a similar spirit, fluorescence resonance energy transfer (FRET) has recently been used to determine reaction rates between membrane-confined receptors and ligands (36). These microscopy experiments can provide estimates of reaction parameters which can then be used to determine if membrane-confined reactions are truly limited by diffusion.

The lifetime of the inactivation state of the enzymes ($1/\mu$) upon catalysis is also an important determi-

nant of ultrasensitivity. Based on the above inequality ($k_- > \mu$), we have estimated that the inactive state should be larger than 1 ms since $k_- \approx 1000\ \mathrm{s}^{-1}$. Detailed analysis of the mechanisms of phosphorylation and dephosphorylation reveals that kinases and tyrosine phosphatases do enter inactive states during catalysis. In the case of kinases, phosphorylation is accompanied by conversion of bound ATP to ADP, and the enzyme remains refractory until the ADP dissociates (22, 23). For tyrosine phosphatases such as CD45, the phosphate group that is removed from the protein is covalently coupled to a cysteine residue in the active site, and the phosphatase remains inactive until this phosphate is removed by hydrolysis (37). The duration of these refractory states is unknown, but because they have been shown to be rate-limiting for catalysis, some information about duration can be inferred from the turnover or k_{cat}, which is readily determined. Since k_{cat} represents the overall rate of all the individual steps in catalysis, including the refractory period, it provides an upper limit for the lifetime of this state (38). Assuming two steps (phosphatase addition/removal followed by enzymatic re-activation), the overall catalytic rate is related to the rate constants of each individual step as $k_{\mathrm{cat}} = k_{\mathrm{r}}\mu/(k_{\mathrm{r}} + \mu)$. Reported k_{cat} values for Lck and CD45 acting on their natural substrates are $\sim$2 s^{-1} (39) and $\sim$50 s^{-1} (40) respectively, consistent with our assumption of inactive states lasting longer than 1 ms. However, further experimental work is needed to determine the precise lifetime of the inactive state.

Implications for membrane-anchored proteins. Regulation of the phosphorylation state of NTRs by extrinsic kinases and phosphatases is poorly understood. As an example, we considered the T cell receptor, which contains 20 sites that are modified by a membrane-anchored kinase (Lck) and phosphatase (CD45). The large number of phosphorylation sites is thought to be important for signal amplification (12) but in this study, we show that multiple sites can also be critical for a switch-like response. A previously described synthetic system (41), whereby a kinase-phosphatase reaction scheme on the T cell receptor has been reconstituted in a non-hematopoietic cell line, can be utilized to explore how multiple sites affects ultrasensitivity. The present work predicts that the Hill coefficient of the kinase-phosphatase dose-response curve will decrease as the number of mutated phosphorylation sites increases, in addition to an overall decrease in the total phosphorylation. An early switch-like response at the level of individual T cell receptors can be useful to discriminate foreign from self ligands and may contribute to the experimentally observed switch-like responses in downstream signaling molecules (2, 6).

Future work. Switch-like responses are likely to be important for other NTRs and other non-receptor membrane-anchored proteins that contain multiple phosphorylation sites. For example, the adaptor protein Linker of activated T cells (LAT) contains 9 sites that are phosphorylated by a Syk family kinase when it is recruited to the plasma membrane (42). A subset of these sites serve as docking sites for a cytosolic molecule known as Grb2, which protects these sites from dephosphorylation and through its interaction with SOS1 can cross-link LAT. A recent theoretical study has highlighted the importance of regulating the phosphorylated state of LAT by showing that the total phosphorylation state of LAT critically determines its oligmeric state (43). Our work has shown that the total phosphorylation state of LAT can be tightly regulated through multiple sites. In our model we did not include the docking of cytosolic molecules and their potential to cross-link membrane-anchored proteins and in the future, it will be important to extend our model to include these features.

We have focused on ultrasensitivity in the total phosphorylation of membrane-anchored proteins using an unstructured (random) phosphorylation scheme. However, some proteins are thought to signal only through specific phosphorylation profiles (e.g. when they are fully phosphorylated) and there are also examples of proteins that exhibit strucutured phosphorylation (e.g. sequential phosphorylation). Previous work has examined these effects (27, 28, 33, 44) and in the future, it will be useful to examine how diffusion-limited

reactions alter these results.

Methods

Spatial simulations using Smoldyn. All spatial simulations are performed using Smoldyn (24), which is a discrete-time continuous-space Monte Carlo agent based simulation tool that accurately captures diffusion, chemical reactions, and spatial confinement (e.g. to a membrane). The algorithm for bimolecular reactions is an essential component of Smoldyn and is based on Smoluchowsky theory of diffusion-limited chemical reactions (24). Binding reactions between an enzyme and substrate take place with a probability of 0.05 at each time step when the two molecules are within the binding radius (5 nm) and upon dissociation of an enzyme-substrate complex (either via k_{off} or k_{r}) the molecules are placed at the binding radius (5 nm). Volume exclusion between enzymes is modeled as effective binary reactions that occur at a specific distance (default exclusion radius is 5 nm) and displaces the molecules to a larger distance (5.5 nm). Decreasing the displacement distance did not alter any of our conclusions but increased simulation times. The area of the simulation domain was taken to be 1 μm^2 with periodic boundary conditions and a fixed time step of 5×10^{-6} s was used. Simulations of the full model (with volume exclusion) required 12 hours of computations per data point using a 2.8 GHz CPU. The Smoldyn script used to generate our results is available upon request.

ACKNOWLEDGEMENTS We thank Louise Johnson and Oreste Acuto for helpful discussions on enzymatic catalysis. We thank Peter Swain, Mohan Malleshaiah, and the anonymous reviewers for helpful comments on the manuscript. This work has been supported by the National Research and Engineering Council of Canada (NSERC) and by the Royal Society through a Newton Fellowship (OD).

References

1. Melen, G. J., S. Levy, N. Barkai, and B.-Z. Shilo, 2005. Threshold responses to morphogen gradients by zero-order ultrasensitivity. *Mol Syst Biol* 1:2005.0028.

2. Altan-Bonnet, G., and R. N. Germain, 2005. Modeling T cell antigen discrimination based on feedback control of digital ERK responses. *PLoS Biol* 3:e356.

3. Tian, T., A. Harding, K. Inder, S. Plowman, R. G. Parton, and J. F. Hancock, 2007. Plasma membrane nanoswitches generate high-fidelity Ras signal transduction. *Nat Cell Biol* 9:905–914.

4. Kim, S. Y., and J. E. Ferrell, 2007. Substrate competition as a source of ultrasensitivity in the inactivation of Wee1. *Cell* 128:1133–1145.

5. Holt, L. J., A. N. Krutchinsky, and D. O. Morgan, 2008. Positive feedback sharpens the anaphase switch. *Nature* 454:353–357.

6. Das, J., M. Ho, J. Zikherman, C. Govern, M. Yang, A. Weiss, A. K. Chakraborty, and J. P. Roose, 2009. Digital signaling and hysteresis characterize ras activation in lymphoid cells. *Cell* 136:337–351.

7. Malleshaiah, M. K., V. Shahrezaei, P. S. Swain, and S. W. Michnick, 2010. The scaffold protein Ste5 directly controls a switch-like mating decision in yeast. *Nature* 465:101–105.

8. Weiss, A., and D. R. Littman, 1994. Signal transduction by lymphocyte antigen receptors. *Cell* 76:263–274.

9. Veillette, A., 2006. Immune regulation by SLAM family receptors and SAP-related adaptors. *Nat Rev Immunol* 6:56–66.

10. Davis, S. J., and P. A. van der Merwe, 2006. The kinetic-segregation model: TCR triggering and beyond. *Nat Immunol* 7:803–809.

11. Lemmon, M. A., and J. Schlessinger, 2010. Cell signaling by receptor tyrosine kinases. *Cell* 141:1117–1134.

12. Guy, C. S., and D. A. A. Vignali, 2009. Organization of proximal signal initiation at the TCR:CD3 complex. *Immunol Rev* 232:7–21.

13. Feinerman, O., R. N. Germain, and G. Altan-Bonnet, 2008. Quantitative challenges in understanding ligand discrimination by alphabeta T cells. *Mol Immunol* 45:619–631.

14. Goldbeter, A., and D. E. Koshland, 1981. An amplified sensitivity arising from covalent modification in biological systems. *Proc Natl Acad Sci U S A* 78:6840–6844.

15. Lauffenburger, D., and J. Linderman, 1993. Receptors: Models for Binding, Trafficking, and Signaling. Oxford University Press.

16. Shoup, D., and A. Szabo, 1982. Role of diffusion in ligand binding to macromolecules and cell-bound receptors. *Biophys J* 40:33–39.

17. Goldstein, B., H. Levine, and D. Torney, 2007. Diffusion limited reactions. *SIAM J. Appl. Math.* 67:1147–1165.

18. Dushek, O., S. Mueller, S. Soubies, D. Depoil, I. Caramalho, D. Coombs, and S. Valitutti, 2008. Effects of Intracellular Calcium and Actin Cytoskeleton on TCR Mobility Measured by Fluorescence Recovery. *PLoS One* 3:e3913.

19. Faeder, J. R., M. L. Blinov, and W. S. Hlavacekc, 2009. Methods in Molecular Biology: Systems Biology, Humana Press, chapter Rule-Based Modeling of Biochemical Systems with BioNetGen.

20. Ciliberto, A., F. Capuani, and J. J. Tyson, 2007. Modeling networks of coupled enzymatic reactions using the total quasi-steady state approximation. *PLoS Comput Biol* 3:e45.

21. Takahashi, K., S. Tanase-Nicola, and P. R. ten Wolde, 2010. Spatio-temporal correlations can drastically change the response of a MAPK pathway. *Proc Natl Acad Sci U S A* 107:2473–2478.

22. Adams, J. A., 2001. Kinetic and catalytic mechanisms of protein kinases. *Chem Rev* 101:2271–2290.

23. Ubersax, J. A., and J. E. Ferrell, 2007. Mechanisms of specificity in protein phosphorylation. *Nat Rev Mol Cell Biol* 8:530–541.

24. Andrews, S. S., N. J. Addy, R. Brent, and A. P. Arkin, 2010. Detailed simulations of cell biology with Smoldyn 2.1. *PLoS Comput Biol* 6:e1000705.

25. Salazar, C., and T. Höfer, 2009. Multisite protein phosphorylation–from molecular mechanisms to kinetic models. *FEBS J* 276:3177–3198.

26. Dushek, O., R. Das, and D. Coombs, 2009. A role for rebinding in rapid and reliable T cell responses to antigen. *PLoS Comput Biol* 5:e1000578.

27. Salazar, C., and T. Höfer, 2007. Versatile regulation of multisite protein phosphorylation by the order of phosphate processing and protein-protein interactions. *FEBS J* 274:1046–1061.

28. Wang, L., Q. Nie, and G. Enciso, 2010. Nonessential sites improve phosphorylation switch. *Biophys J* 99:L41–L43.

29. Liu, X., L. Bardwell, and Q. Nie, 2010. A combination of multisite phosphorylation and substrate sequestration produces switchlike responses. *Biophys J* 98:1396–1407.

30. Lenz, P., and P. S. Swain, 2006. An entropic mechanism to generate highly cooperative and specific binding from protein phosphorylations. *Curr Biol* 16:2150–2155.

31. Ferrell, J. E., and E. M. Machleder, 1998. The biochemical basis of an all-or-none cell fate switch in Xenopus oocytes. *Science* 280:895–898.

32. Markevich, N. I., J. B. Hoek, and B. N. Kholodenko, 2004. Signaling switches and bistability arising from multisite phosphorylation in protein kinase cascades. *J Cell Biol* 164:353–359.

33. Thomson, M., and J. Gunawardena, 2009. Unlimited multistability in multisite phosphorylation systems. *Nature* 460:274–277.

34. Sprague, B. L., R. L. Pego, D. A. Stavreva, and J. G. McNally, 2004. Analysis of binding reactions by fluorescence recovery after photobleaching. *Biophys J* 86:3473–3495.

35. Dushek, O., R. Das, and D. Coombs, 2008. Analysis of membrane-localized binding kinetics with FRAP. *Eur Biophys J* 37:627–638.

36. Huppa, J. B., M. Axmann, M. A. Mrtelmaier, B. F. Lillemeier, E. W. Newell, M. Brameshuber, L. O. Klein, G. J. Schtz, and M. M. Davis, 2010. TCR-peptide-MHC interactions in situ show accelerated kinetics and increased affinity. *Nature* 463:963–967.

37. Barford, D., A. K. Das, and M. P. Egloff, 1998. The structure and mechanism of protein phosphatases: insights into catalysis and regulation. *Annu Rev Biophys Biomol Struct* 27:133–164.

38. Fersht, A., 1999. Structure and mechanism in protein science: A guide to enzyme catalysis and protein folding. W H Freeman and Company.

39. Ramer, S. E., D. G. Winkler, A. Carrera, T. M. Roberts, and C. T. Walsh, 1991. Purification and initial characterization of the lymphoid-cell protein-tyrosine kinase p56lck from a baculovirus expression system. *Proc Natl Acad Sci U S A* 88:6254–6258.

40. Felberg, J., and P. Johnson, 1998. Characterization of recombinant CD45 cytoplasmic domain proteins. Evidence for intramolecular and intermolecular interactions. *J Biol Chem* 273:17839–17845.

41. van Oers, N. S., B. Tohlen, B. Malissen, C. R. Moomaw, S. Afendis, and C. A. Slaughter, 2000. The 21- and 23-kD forms of TCR zeta are generated by specific ITAM phosphorylations. *Nat Immunol* 1:322–328.

42. Samelson, L. E., 2002. Signal transduction mediated by the T cell antigen receptor: the role of adapter proteins. *Annu Rev Immunol* 20:371–394.

43. Nag, A., M. I. Monine, J. R. Faeder, and B. Goldstein, 2009. Aggregation of membrane proteins by cytosolic cross-linkers: theory and simulation of the LAT-Grb2-SOS1 system. *Biophys J* 96:2604–2623.

44. Gunawardena, J., 2005. Multisite protein phosphorylation makes a good threshold but can be a poor switch. *Proc Natl Acad Sci U S A* 102:14617–14622.

Tables

Table 1: Parameter definitions for the two-step ODE model.

Parameter	Description	Units
k_+	Diffusion-limited on-rate	$\mu\text{m}^2\ \text{s}^{-1}$
k_-	Local diffusion rate ($k_- = k_+/A$)	s^{-1}
k_{on}	Bimolecular on-rate	$\mu\text{m}^2\ \text{s}^{-1}$
k^*_{on}	Local on-rate ($k^*_{\text{on}} = k_{\text{on}}/A$)	s^{-1}
k_{off}	Unbinding rate	s^{-1}
k_{r}	Modification rate	s^{-1}
μ	Reactivation rate	s^{-1}
A	Encounter area ($A = \pi s^2$)	μm^2
s	Binding radius	μm

Figure Legends

Figure 1: Schematic of the two-step model coupled to multisite phosphorylation. A) We model the interaction between membrane anchored multisite proteins (blue) and membrane anchored enzymes (red). The rate at which an enzyme forms an encounter-complex (centre) with the substrate is determined by the diffusion-limited on-rate (k_+) multiplied by the free enzyme concentration (X). Within the encounter-complex, the enzyme and substrate can bind or move apart with first order rates k^*_{on} and k_-, respectively. We assume a random phosphorylation scheme and therefore the effective binding rate is proportional to k^*_{on}, the single-site binding rate, multiplied by the number of (un)phosphorylated sites. Note that the microscopic rates, k^*_{on} and k_-, are on the scale of a single substrate and enzyme but are directly proportional to the macroscopic rates $k^*_{\text{on}} = k_{\text{on}}/A$ and $k_- = k_+/A$, where k_{on} is the bimolecular on-rate and A is the approximate area of the substrate. When in complex (right), the enzyme may catalyze a reaction and unbind (k_{r}, not shown) or unbind (k_{off}) and in both reactions the enzyme and substrate return to the encounter complex (centre). B) Overhead view of the three states in panel A with approximate scales. C) In the most general model we consider, upon catalysis the enzyme becomes inactive for a short period ($1/\mu$) before further catalysis may take place. Therefore upon catalysis the enzyme may diffuse away (k_-) or re-activate (μ).

Figure 2: Ultrasensitivity in multisite phosphorylation arising from diffusion-limited reactions and enzymatic inactivation. We compute the total phosphorylation state of the substrate (equation 2) at equilibrium as a function of the total kinase (E) and phosphatase (F) concentrations using the two step model (Fig. 1, main text) for 1-20 phosphorylation sites (colored lines). All calculations are performed in the limit where enzymes saturate the substrate. A) In the reaction-limited regime ($k_{\text{on}} = k_+/100$) we obtain the established result of small Hill numbers and find that increasing the number of sites does not produce ultrasensitivity. B) In the diffusion-limited regime ($k_{\text{on}} = 100k_+$), local saturation effectively produces a processive scheme whereby local rebinding allows multiple modifications during a single enzyme-substrate encounter. C-D) Introducing an enzymatic refractory state ($\mu = 1$ s^{-1}) attenuates processivity by decreasing the probability of rebinding but only in the diffusion-limited regime (panel D) is ultrasensitivity observed due to local enzymatic saturation. Arrow indicates direction of increasing phosphorylation sites and insets quantify the Hill number. Parameters: $k_+ = 0.1$ μm$^2/s$ (diffusion-limited), $k_+ = 10$ μm$^2/s$ (reaction-limited), $k_{\text{off}} = 1$ s^{-1}, $k_{\text{r}} = 0.1$ s^{-1}, $A = 0.01^2$ μm^2 (encounter-area), $k^*_{\text{on}} = k_{\text{on}}/A$, and $k_- = k_+/A$.

Figure 3: Parameter regimes supporting ultrasensivity. Heat maps of the Hill number are shown for a 20-site protein as a function of A) μ vs. k_-, B) k^*_{on} vs. k_-, and C) k_{off} vs. k_{r}. Panels A and B show ultrasensivity in regimes where enzymes become locally saturated ($k_- < k^*_{\text{on}}$) and act distributively ($\mu < k_-$). Therefore ultrasensivitity is supported when $k^*_{\text{on}} > k_- > \mu$. Default parameters: $k_{\text{on}} = 10$ μm^2/s, $k_+ = k_{\text{on}}/100$ μm^2/s, $k_{\text{off}} = 1$ s^{-1}, $k_{\text{r}} = 0.1$ s^{-1}, $A = 0.01^2$ μm^2 (encounter-area), $k^*_{\text{on}} = k_{\text{on}}/A = 10^5$ s^{-1}, $k_- = k_+/A = 10^3$ s^{-1}, and $\mu = 1$ s^{-1}.

Figure 4: Explicit spatial simulations recapitulate results obtained using the two-step ODE model and reveal the importance of volume exclusion. A) The normalized total phosphorylation of the substrate (equation 2) at equilibrium as a function of the total kinase (E) and phosphatase (F) concentrations using spatial simulations in two-dimensions with volume exclusion and enzymatic inactivation for the indicated number of phosphorylation sites. Each simulations is performed with 1 substrates and 100 enzymes in the simulation domain and therefore enzymes globally saturate the substrate. B) Hill numbers as a function of the number of phosphorylation sites for the simulations in panel A (blue), for the case when volume exclusion is removed (green), for short refractory periods (red), and for the reaction-limited regime (orange). C) The dose-response for the 20 site substrate for different exclusion radii (fitted Hill numbers are indicated). Note that the binding radius is fixed at 5 nm and therefore an exclusion radius larger than 10 nm allows only a single enzyme to interact with the substrate. All simulations are performed using Smoldyn (24). Parameters: volume exclusion radius is 5 nm (default) or 0 nm without volume exclusion; binding radius is fixed at 5nm; diffusion coefficient for enzymes and substrate is 0.01 $\mu\text{m}^2/s$ (default) or 10 $\mu\text{m}^2/s$ for the reaction-limited simulation; $\mu = 1\ \text{s}^{-1}$ (default) or $\mu = 10000\ \text{s}^{-1}$ for the short refractory period simulation; $k_\text{r} = 0.1\ \text{s}^{-1}$; $k_\text{off} = 1\ \text{s}^{-1}$; see Methods for additional details. The total phosphorylation state of the receptor is obtained by averaging the simulation for 1500 s at each E/F ratio.

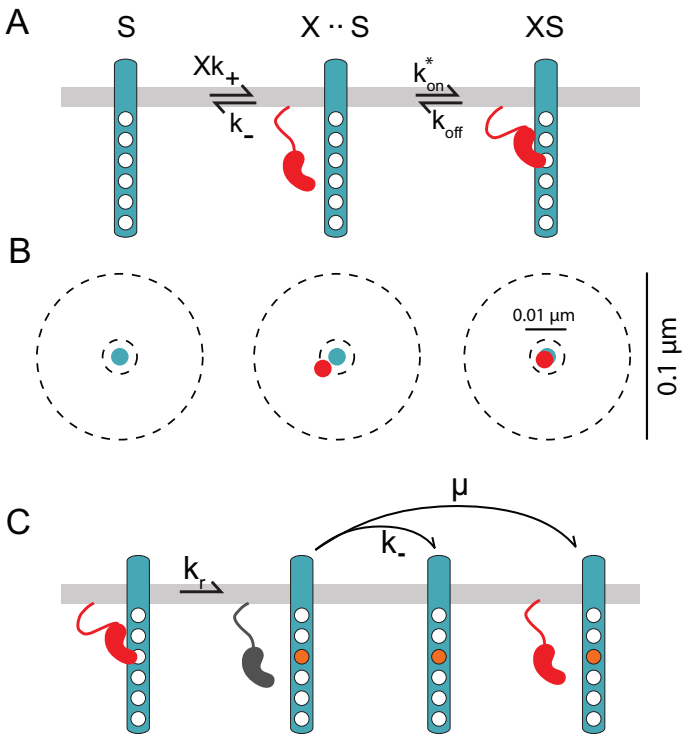

Fig 1:

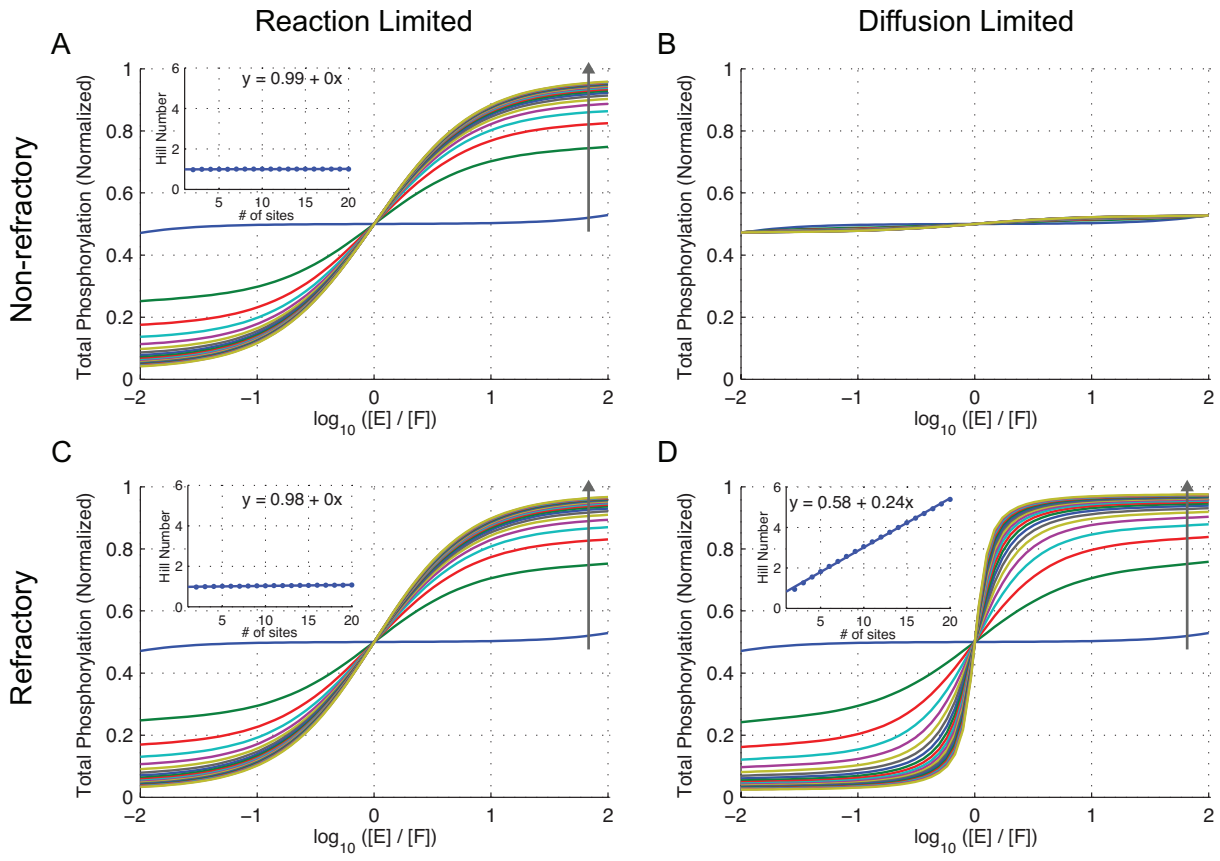
Reaction Limited
Diffusion Limited
A
B
C
D
Non-refractory
Refractory
Total Phosphorylation (Normalized)
log10 ([E] / [F])
Hill Number
# of sites
y = 0.99 + 0x
y = 0.98 + 0x
y = 0.58 + 0.24x

Fig 2:

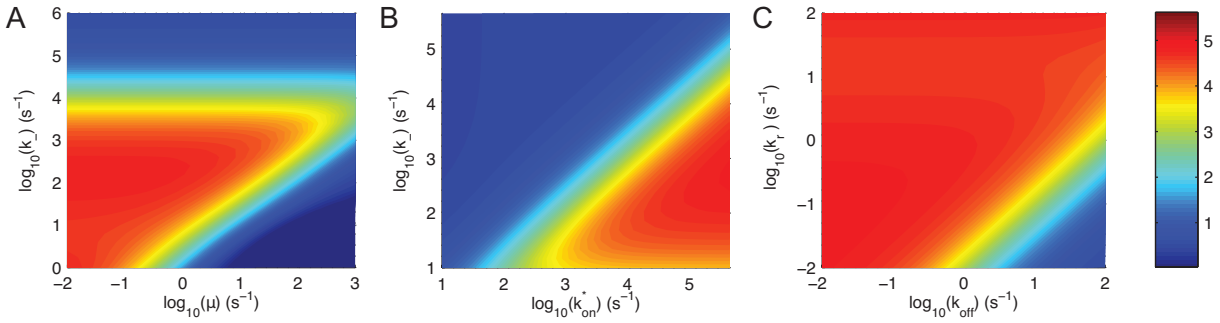

Fig 3:

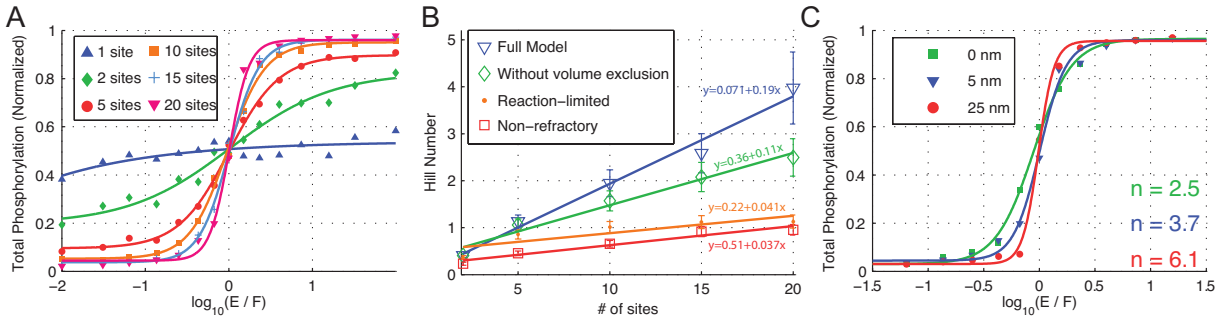
A
1 site
10 sites
2 sites
15 sites
5 sites
20 sites
Total Phosphorylation (Normalized)
log10(E / F)
B
Full Model
Without volume exclusion
Reaction−limited
Non−refractory
y=0.071+0.19x
y=0.36+0.11x
y=0.22+0.041x
y=0.51+0.037x
Hill Number
# of sites
C
0 nm
5 nm
25 nm
n = 2.5
n = 3.7
n = 6.1
Total Phosphorylation (Normalized)
log10(E / F)

Fig 4:

1:

2:

3: